Hindawi
Journal of Sensors
Volume 2022, Article ID 1048914, 12 pages
https://doi.org/10.1155/2022/1048914

Research Article

Analysis of Dynamic System of Exercise Load Condition Monitoring Based on Characteristic Parameters

Yunlan Ren[1] **and Shang Wu**[2]

[1]*School of Applied Engineering Henan University of Science and Technology, Zhengzhou Henan 472000, China*
[2]*School of Police Sport Henan Police College, Zhengzhou Henan 450046, China*

Correspondence should be addressed to Shang Wu; 20170472@hnp.edu.cn

Received 10 November 2021; Revised 10 January 2022; Accepted 17 January 2022; Published 14 February 2022

Academic Editor: Gengxin Sun

According to the algorithm of time difference and threshold value, this paper selects the more valuable data for motion state recognition and selects the characteristics, respectively selects the data of the combined acceleration and the combined angular velocity, and uses the data of the pitch angle and the roll angle more novelly. In the aspect of data preprocessing, the sliding segmentation window method is used for feature processing, and the time domain and frequency domain features of the data are extracted. A total of 108 dimensional features are extracted. In order to improve the calculation performance, PCA technology is used for data dimensionality reduction. In this paper, we collected data on changes in physiological parameters of 24 experimenters before and after exercise, collected 14 self-evaluated severely fatigued volunteers and self-evaluated severely stressed volunteers' resting heart rate and blood pressure data as unhealthy data samples, and collected physiological data of 14 healthy experimenters as unhealthy data samples. For healthy samples, three sets of experiments were set up to analyze the changes of exercise heart rate, exercise blood pressure and exercise body temperature, and the effectiveness of fusion of physiological data to improve the performance of exercise recognition and the analysis of the health status of physiological parameters that introduce exercise interference. The experimental results show that during exercise, monitoring changes in systolic blood pressure is more meaningful than monitoring changes in diastolic blood pressure; it verifies the effectiveness of improving the performance of exercise recognition by fusion of physiological parameters. The addition of physiological data can effectively improve the recognition rate of exercise. The recognition rate has been increased from 93.7% to 96.3%; the effectiveness and applicability of the algorithm in this paper are analyzed through design experiments, and the results show that the recognition accuracy of the algorithm in this paper is above 87%. This result has a good classification recognition rate for a small sample.

1. Introduction

With the continuous improvement of living standards, people's living habits and eating habits are also changing. Excessive diet, intake of high-calorie food, and lack of exercise due to staying indoors for a long time are increasing, causing the human body to consume too much energy every day, leading to diseases such as obesity, high blood pressure, and hyperlipidemia [1]. Developing a healthy diet and taking an active part in outdoor activities can not only enhance the body's immunity but also consume excess energy, so that the body's energy supply and demand can reach a balance [2]. Monitoring the daily exercise status of the human body can guide people to formulate a healthy and reasonable diet plan, rationally arrange daily exercise, and improve people's healthy living standards [3]. There are many types of daily activities of the human body, including running, walking, going up and down the stairs, sitting down, standing, and many other exercise methods. The energy consumption relationship corresponding to these different daily exercises is also different. Therefore, it is very important to monitor and identify these daily exercises, and it is also the main research topic of many researchers at present [4].

The acceleration phenomenon has always existed in human body movement; for example, daily human body movements such as washing face, brushing teeth, walking, running, and riding a bicycle will produce corresponding acceleration. The use of acceleration to monitor human motion status has received extensive attention from domestic and foreign researchers [5]. The acceleration signal is the corresponding action signal generated by the body movement in the daily life of the human body. By effectively processing this signal, it can be judged what kind of action the human body has made [6]. With the continuous improvement of microelectronic system technology, acceleration sensors are becoming smaller and cheaper, and they have been widely embedded in mobile phone devices, notebooks, electronic game consoles, etc., and are based on acceleration sensors [7]. Various studies provide a broader platform. The human action recognition mechanism and fall detection algorithm proposed in this paper are based on a single acceleration sensor [8]. Most of the current popular smartphones and other devices have a single acceleration sensor embedded, so the research in this paper has a certain practical value [9].

Wearable health monitoring devices are often greatly affected by the state of human movement. Through the identification and analysis of different exercise states, the real health conditions contained in the health data can be better mined. Recognition of human motion status has development prospects in many fields such as health field, medical monitoring, fall monitoring, competitive sports, and indoor positioning. In daily life, different motion states will produce different accelerations. Accurate identification of individual motion states can be achieved by acquiring acceleration signals in different motion states and performing corresponding preprocessing and feature identification. The rapid development of artificial intelligence technology provides a strong support for solving feature recognition and improving the ability to identify behaviors autonomously. Various intelligent mobile terminal devices that are widely used contain a wealth of sensors, which provide the possibility for convenient monitoring of physiological parameters, but the monitoring data is often greatly affected by the state of human movement. Through the identification and analysis of different motion states, the real physiological information contained in the monitoring data can be better mined.

This paper uses the random forest classification algorithm to classify the movement state. Using variable-scale sliding window segmentation technology, 27 time-domain and frequency-domain features of total acceleration, total angular velocity, pitch angle, and roll angle are extracted, respectively. A total of 108 features are extracted for each action, and the PCA algorithm is used to do feature extraction. This paper collects data from 24 experimenters and analyzes the changes in exercise heart rate, blood pressure, and body temperature. The results show that human body sweat evaporation and other factors lead to insignificant changes in human body temperature monitoring values. Exercise blood pressure changes according to a certain rule. The above reflects the health of the human body. In predicting the health status based on the physiological data of the monitored human body's real-time exercise status, the physiological parameter health status analysis that introduces exercise interference can be used to distinguish the changes in the physiological parameters caused by the individual exercise and the changes caused by the abnormal physical health of the individual. After counting the changes in blood pressure and heart rate of 24 experimenters, it can be concluded that after 5 minutes of vigorous exercise, most of the experimenters' systolic blood pressure will increase to a certain extent, but the diastolic blood pressure basically remains unchanged or has a small extent decrease; the heart rate rises sharply. Therefore, during exercise, it is more meaningful to monitor changes in systolic blood pressure than to monitor changes in diastolic blood pressure. Exercise can lower the body's diastolic blood pressure. In terms of diastolic blood pressure monitoring, the overall stability of diastolic blood pressure of female experimenters is higher than that of men. Changes in blood pressure during exercise can reflect the health of the human body to a certain extent, and the changes are also related to the height and weight of the experimenter.

2. Related Work

The multisensor strategy is to place acceleration sensors, gyroscopes, height sensors, air pressure sensors, skin conductivity sensors, heart rate sensors, etc., on the head, wrist, waist, ankle, sole, or skeletal muscle joints of the human body. It collects data collaboratively and uploads data to the analysis platform in real time through data transmission equipment such as Bluetooth. The advantage of the multipoint arrangement is that detailed and comprehensive data can be obtained, and the corresponding algorithm can be used to accurately identify the complex action process. It is often used in the fields of game modeling, athlete's posture analysis, and training correction. Judging from commercialization results, there are many successful cases [10]. Taking wearable devices as an example, wristbands with pedometer functions are all the rage. The main implementation mode of this type of product does not only analyze the data of the motion sensor alone but also analyzes the mileage and step frequency through the GPS function of the mobile phone to compensate for the step error [11]. Accelerometers, gyroscopes, and magnetometers are generally integrated into mobile phones. In response to the upsurge of motion recognition research, many companies have introduced special equipment for data sampling, such as Microsoft's band2 [12].

Relevant scholars observe the impact of a six-week virtual reality exercise experiment on cognitive ability [13]. In the experiment, six weeks of virtual reality exercises such as stretching exercises, archery exercises, and balance exercises was used. The 32-lead Brain Vision Analyzer produced by BP in Germany was used for ERP P300 evaluation. The results showed that six weeks of virtual reality exercises was used during exercise. Undergraduates' cognitive ability has a certain selective influence, and it is believed that these selective changes should be adaptive changes to the exercise style [14]. Related scholars have observed the effect of high-

intensity interval training on the ability of adolescents to exercise control [15]. Using six weeks of high-intensity interval training or choosing aerobic continuous training can significantly shorten the stroop reaction time of young children, but the effect of the high-intensity interval training group is significantly better than that of continuous aerobic training.

The single-sensor strategy undergoes data processing and algorithm recognition and outputs the judgment result of the motion state. The data processing capacity of a single sensor is relatively small, and although it cannot recognize complex human movements, the recognition of walking, running, falling, and other movements can reach a high degree of accuracy. It is mainly used in the fields of elderly fall detection, medical rehabilitation, exercise assistance, and other fields.

In the research of motion recognition, the preprocessing of accelerometer data mainly includes data transformation, filtering, and sample collection [16]. The main purpose of data transformation is to decompose or merge the original data that is not convenient for analysis to obtain target values that are beneficial for analysis or feature extraction. At present, the main analysis object of domestic and foreign researchers is the resultant acceleration derived from the three-axis acceleration, and a small number of studies use the raw data of the three-axis acceleration for comprehensive analysis [17]. For data filtering, some researchers have analyzed the influence of median filtering, moving average filtering, and Kalman filtering on the signal [18]. At present, the windowing method is commonly used at home and abroad to process acceleration sampling data. Researchers mainly conduct testing and research on the time length and overlap ratio of windows to find the best window setting form [19]. Other data set extraction methods include the key event cut-off method, which is mainly a supplement to the continuous recognition of the window method. This method selects certain feature points as the settlement signal for the feature value extraction of the window data, such as points with a higher rate of change.

The motion recognition algorithm is the core of motion recognition research [20]. The algorithms used by domestic and foreign researchers mainly include naive Bayes algorithm, K-nearest neighbor algorithm, threshold algorithm, decision tree algorithm, random forest algorithm, SVM support vector machine algorithm, and BP neural network [21]. Among them, the decision tree algorithm is actually a tree topology representation of the threshold algorithm, and the entropy gain calculation of the split node is more reliable than a single threshold. The random forest algorithm has absorbed the naive Bayesian algorithm's thoughts on the probability processing of classified events and the advantages of a simple and efficient decision tree algorithm [22]. The naive Bayes algorithm is highly efficient and concise, and the time complexity and space complexity of the program are extremely low. However, the calculation of its prior probability requires a lot of statistical work. At present, with the increasing popularity of machine learning and artificial intelligence, more researchers use the BP neural network. The BP neural network has many advantages. Related scholars use context-aware technology to identify feedback and optimize control of robot motion processes [23]. However, its algorithm has high complexity, high requirements for system hardware resources, and slow speed, and the training results are affected by many factors. At present, the relevant literature is only seen in laboratory simulations, and no mature products have been launched [24].

3. Method

3.1. The Overall Architecture of the Monitoring Dynamic System. According to functional requirements, the system needs the implementation of the data acquisition module, low power consumption module, positioning module, system alarm module, remote communication module, and other software. The working mode of the dynamic system of exercise load status monitoring is shown in Figure 1.

After the system switch is turned on and powered on, in the main function, initialize the clock, USART, timer 2, timer 7, IIC, MPU9250, MAX30102, SD card, and open the MTK serial port to communicate with the remote server. After the connection is successful, the system obtains the initial data. If the system detects that the user is not exercising, the heart rate is normal, and there is no abnormality after 3000 times (30 s) of information monitoring, it will enter the low power consumption mode, and no exercise status recognition will be performed at this time; if the user is detected in motion state, the MPU9250 interrupt pin will wake up the STM32F4. At this time, the system enters the high-speed motion mode. According to the acceleration, angular velocity, attitude angle, and time difference data, it recognizes the user's walking, running, sitting, standing, falling danger, and falling. When the result is recognized, a flag bit specified by the system will be returned, then send it to MTK through the serial port, and MTK will broadcast the corresponding action voice. At the same time, MTK will package the corresponding signs of the corresponding action information, positioning information, power, and other information into the form of BSN data packets and upload them to the server. The BSN data packet format is a data transmission protocol defined by humans. If the user has a fall or an abnormal heart rate, the system will give an alarm and send its location information to the guardian in order to get timely help. If the user is rescued in time and the alarm state is released (press the release alarm button), then the system will continue to enter the motion monitoring mode and continue to work. The data package in the upload server mode is shown in Table 1.

3.2. Feature Extraction and Selection. There are many features that can be extracted by motion state recognition, which are mainly divided into time domain and frequency domain features. Time domain features (TDF) mainly refer to the time-related features that the signal has during the change of the signal with time; frequency domain features (FDF) are mainly used to find some periodic signals in the signal, and the frequency domain is mainly calculated by Fast Fourier Transform (FFT). Taking the resultant

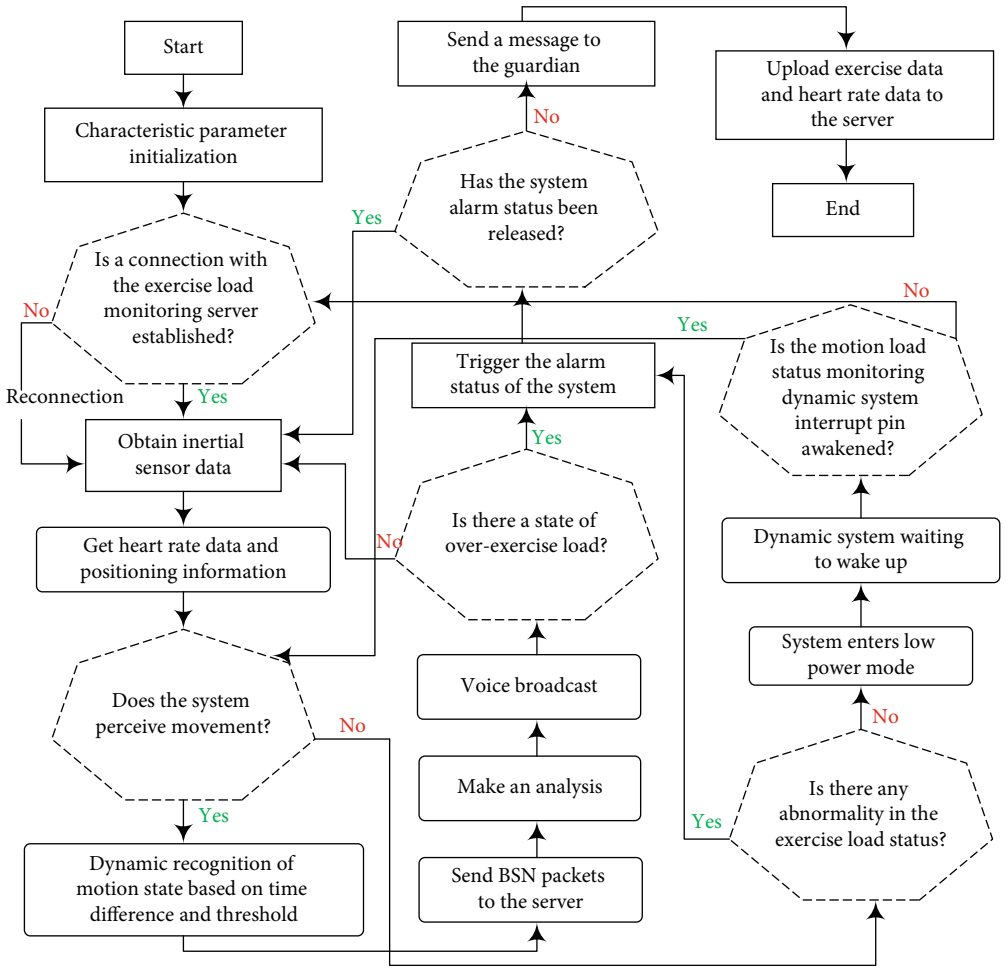

Figure 1: Work flow chart of the dynamic system for monitoring the exercise load state.

acceleration data as an example, the features that can be extracted are shown in Figure 2.

The mean value is often used to identify sitting and standing states, while the root mean square is used to distinguish walking patterns, and the signal amplitude area is used to distinguish motion to determine when the subject is engaged in activity and when in static state. Energy and entropy are used to distinguish different types of daily life states. The signal amplitude vector is used to indicate the degree of exercise intensity, and it is an important indicator of fall detection. Standard deviation has also been widely used for activity classification.

For a given set of signals: $Y = \{y1, \cdots, yn\}$, we perform FFT transformation, where Fi is the ith component of the Fourier transform of Y. The calculation method of each feature is as follows.

The standard deviation is

$$\text{std} = \left[\frac{1}{n}\sum_{i=1}^{n}(y_i - \text{mean})^2\right]^{1/2}. \quad (1)$$

Table 1: Upload data package in server mode.

Frame header	BSN
System ID	SIM card number
1	Battery voltage level
2	Exercise status
3	GPS positioning information
4	Base station location information
5	WIFI location information
6	Battery voltage
End of frame	@

The energy is

$$\text{Energy}(Y) = \frac{1}{n}\prod_{i=1}^{n}F_i^2. \quad (2)$$

The calculation methods of mean uamp, standard deviation σamp, skewness γamp, and kurtosis ηamp of amplitude

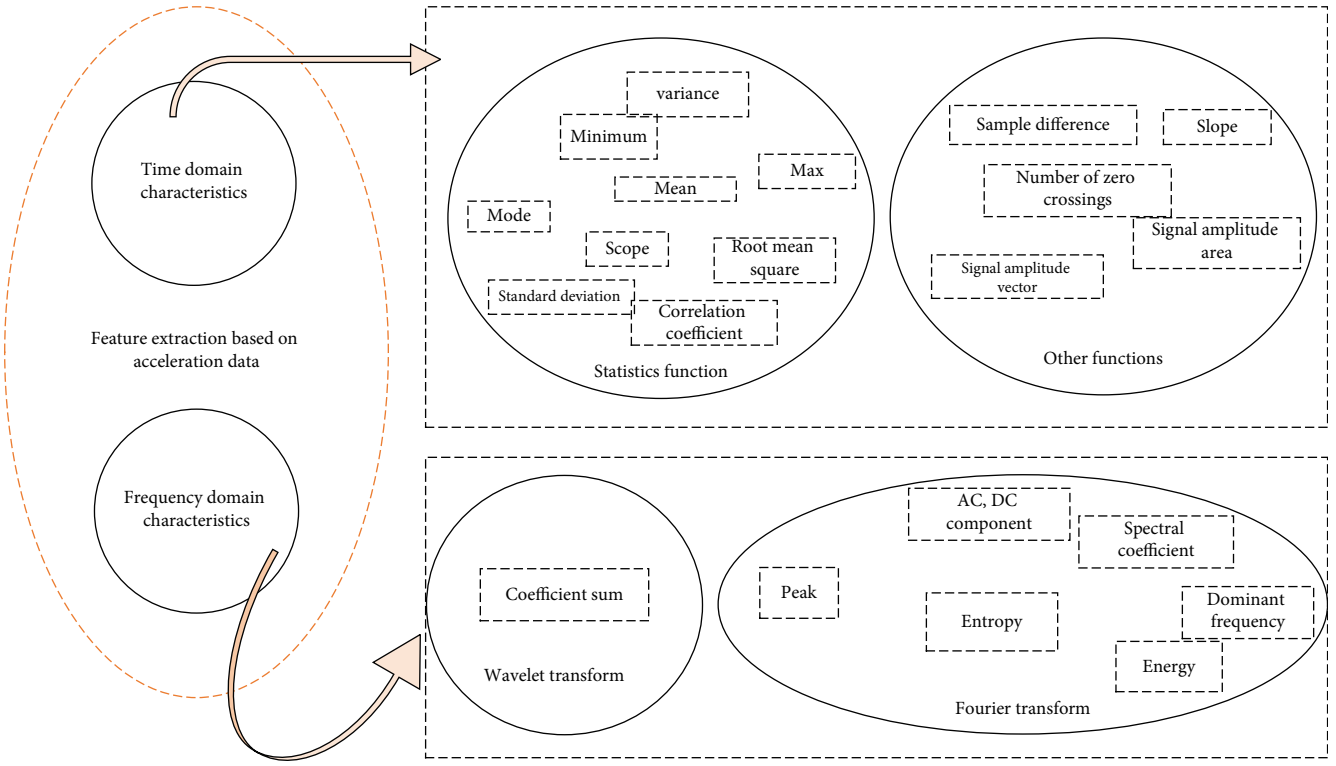

Figure 2: Schematic diagram of feature extraction of acceleration data.

statistical characteristics are as follows:

$$\text{uamp} = \frac{1}{M-1}\prod_{i=0}^{M-1}[D(i)\cdot D(i+1)], \tag{3}$$

$$\sigma\text{amp} = \left\{\frac{1}{M-1}\prod_{i=0}^{M-1}[D(i)\cdot D(i+1) - \text{uamp}]^2\right\}^{1/2}, \tag{4}$$

$$\gamma\text{amp} = \frac{1}{M-1}\prod_{i=0}^{M-1}\left[D(i)\cdot D(i+1) - \frac{\text{uamp}}{\sigma\text{amp}}\right]^3, \tag{5}$$

$$\eta\text{amp} = \frac{1}{M-1}\prod_{i=0}^{M-1}\left[\frac{D(i)\cdot D(i+1)}{\sigma\text{amp} - \text{uamp}} - 1\right]^2. \tag{6}$$

This paper extracts the time-domain and frequency-domain features of the combined acceleration, combined angular velocity, pitch angle, and roll angle. 27 features are extracted from each type of data. A total of 108 features are extracted for each action, and these features are combined into feature vectors. Each row represents a sample, and each column represents a feature, which constitutes a data set for motion state recognition.

3.3. Use PCA for Data Feature Extraction. After the data is preprocessed and feature extracted, it is necessary to reduce the dimensions of the data features, retain the most important features, and input the machine learning algorithm for training, which can reduce the computational overhead of the algorithm and make the data set easier to use. Dimensionality reduction is a way to retain some of the most important features of high-dimensional data and remove unimportant features and noise, so as to achieve the purpose of improving the data processing speed.

Principal component analysis is a type of unsupervised dimensionality reduction method. Its goal is to reduce a set of N-dimensional vectors to K-dimensional and to ensure that the variance of any two vectors is as large as possible. In order to ensure that the two vectors represent as much of the original information as possible, there should be no linear correlation between the vectors. This requires the selection of K orthogonal features, the principal components. It is a k-dimensional feature reconstructed on the basis of the original n-dimensional feature. This is to find a set of mutually orthogonal principal components in turn from the original space.

The first principal component selects the direction with the largest variance in the original data, and the second principal component selects the direction with the second largest variance in the data. For the third principal component, we choose the plane with the largest variance on the planes orthogonal to the directions of the first and second principal components. By analogy, K principal components are selected.

The variance is mainly contained in the K principal components, and the variance of the remaining principal components is almost zero. Therefore, we use K principal components to transform the original data into a new space, realizing dimensionality reduction of data features.

Through PCA dimensionality reduction, the percentage of the total variance of each principal component in the

feature matrix can be calculated, that is, the contribution rate. The percentage of the total variance of the first few principal components is called the cumulative contribution rate. In general, the first few principal components whose cumulative contribution rate reaches 90% are selected to ensure that all important feature information is included. In addition, the included noise and irrelevant information are removed to make the data clearer.

3.4. Recognition of Exercise Load State Based on Random Forest. This paper chooses the random forest (RF) classifier as the algorithm of motion state recognition. Random forest is an ensemble learning algorithm, it belongs to the bagging type, and the bagging structure is shown in Figure 3. It mainly combines multiple weak classifiers, and each classifier votes to get the final result. A random forest is actually a classifier with multiple decision trees, and each decision tree is not related. When the data to be tested enters the random forest, each tree in it will be classified, and the output category is determined by the mode of the output results of some trees; the final classification result in all decision trees is the final classification. Because "random" can make it have the ability to resist overfitting and "forest" makes it more accurate, it can achieve a good classification effect.

Suppose that the set S contains n different samples $\{x1, x2, \cdots, xn\}$. If one sample is randomly selected from the set S each time and it is sampling with replacement, a total of n times are drawn, and the new set $S*$ is formed. Then, the probability that a certain sample $xi\,(i = 1, 2, \cdots, n)$ is not included in the set $S*$ is

$$p = \left(\frac{1-1}{n}\right)^{n}. \tag{7}$$

When n tends to infinity,

$$\lim_{n\Rightarrow+\infty} p = \lim_{n\Rightarrow+\infty}\left(\frac{1-1}{n}\right)^{n+1} = e^{-1} \longrightarrow 0.368. \tag{8}$$

Therefore, although the total number of samples in the new set is equal to that in the original set, the new set is obtained by randomly sampling S samples with replacement n times, so it may have duplicate samples. If the duplicate samples are removed, the new set contains 0.63 samples in the original set.

The random forest algorithm is based on the bootstrap method of resampling to generate multiple training sets, and when constructing the decision tree, a method of randomly selecting a split attribute set is used. When inputting the feature matrix into the classifier, each sample in the training set and the test set needs to be labeled with a corresponding label for subsequent recognition.

4. System Test and Result Analysis

4.1. Data Preprocessing. The data includes three-axis acceleration, three-axis angular velocity, three-axis magnetometer, and attitude angle. The motion data used in this article mainly includes the combined acceleration, combined angular velocity, pitch angle, and roll angle, which can better reflect the human body's movements. However, the data collected is a period of time, and the amount of information is relatively large, which is not conducive to subsequent feature extraction. Therefore, window segmentation is required; that is, given a time series and a limited sample set characterized by time points, the sample set is divided into segments (windows) of continuous samples between two time points a and b. These two time points are internally homogeneous for the program.

How to determine the segmentation window is a key issue when performing window segmentation. For example, activities with a relatively short duration, such as sitting down, cannot be effectively recognized if the window is too long or too short. In fact, many classification errors in motion state recognition are caused by improper selection of the size of the segmentation window. If the window is too short, it may not cover the span of an action. If the window is too long, it may overlap two unrelated activities. This article uses sliding window segmentation technology and takes different sliding windows F according to different actions. Each sliding step $F/2$ means that each window segmentation will have a 50% overlap rate for the previous time window. This ensures that each action has better integrity. In this article, according to the different actions and the collected data analysis, the window chooses 100 and 200, such as falling, sitting, and standing. It takes about 2 s for the completeness of the data, so the segmentation window is selected as 200. It takes about 1 s to go upstairs, go downstairs, and stand still, so the split window is selected as 100, as shown in Figure 4. It can be seen that when the sliding window is selected as 100, the integrity of the action will not be destroyed.

4.2. Exercise Heart Rate and Exercise Blood Pressure Monitoring Test. Before the measurement, the experimenter should avoid strenuous exercise, keep calm, and conduct the experiment in a quiet environment. The experimenter needs to fill in basic personal information, including gender, age, height, and weight, and needs to clearly inform whether he has cardiovascular-related diseases and whether he has any medication records in the near future. After completing the basic information collection, it needs to wear the collection equipment correctly. We collect ECG signals, PPG signals, and blood pressure signals. After wearing the equipment correctly, first, we ask each experimenter to stay calm and maintain a resting state for 1 minute. After 1 minute, we record the physiological data within one minute, in which blood pressure is measured three times repeatedly, and use an electronic thermometer to measure the experimenter's resting state before exercise.

After the initial data collection is completed, take off the measurement equipment worn and exercise vigorously for 5 minutes in a running state. After finishing the exercise, the experimenter wears the measuring equipment again and immediately starts data collection in the same way as the initial data collection. We record the changes of data every 2 minutes until the measured values are basically stable.

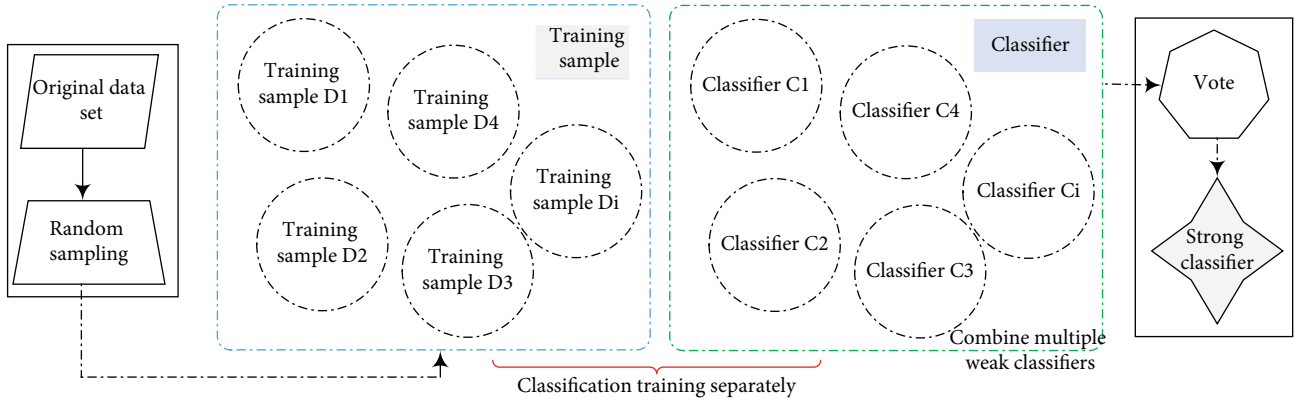

Figure 3: Bagging structure.

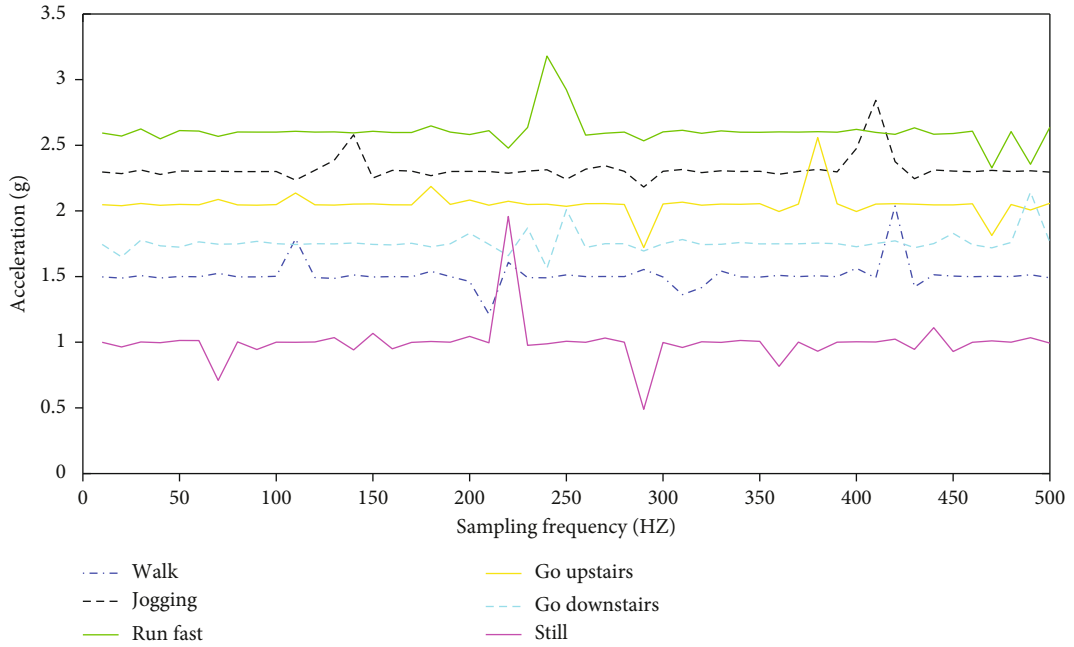

Figure 4: The acceleration of the sliding window segmentation when the overlay rate is 50% and the window is 100.

Table 2: Measurement data of the first experimenter.

Motion state	HR (bpm)	T (°C)	SBP (mm Hg)	DBP (mm Hg)
Resting state before exercise	90.2	36.1	113.1	69.1
	93.3	35.9	111.4	68.1
	91.0	36.2	115.1	68.3
After exercise	119.1	36.3	129.3	67.1
	117.4	36.1	128.1	65.3
	118.1	36.4	129.3	68.1
Resting after exercise	109.1	36.4	116.1	71.2
	105.0	36.3	114.1	69.3
	108.1	36.5	118.3	70.1

This section focuses on the analysis of the changes in the blood pressure of the experimenter before and after exercise. A total of 24 experimenter sample data were collected, and the measurement data of one experimenter was randomly selected as an example for analysis and explanation. Table 2 shows the systolic blood pressure, diastolic blood pressure, and heart rate of the first experimenter before and after exercise and after recovery. It can be seen from Table 1 that after 5 minutes of strenuous exercise, both blood pressure and heart rate values will change significantly, and after 10 minutes of rest recovery, the measured data basically return to a stable state.

After statistical analysis, it is found that using a forehead thermometer to measure human body temperature before and after exercise, the value of the change is small. The main reason is that the selected experimental environment is relatively open, the body surface temperature is greatly affected by the environment, and the human body sweat evaporation and other factors lead to the human body temperature. The

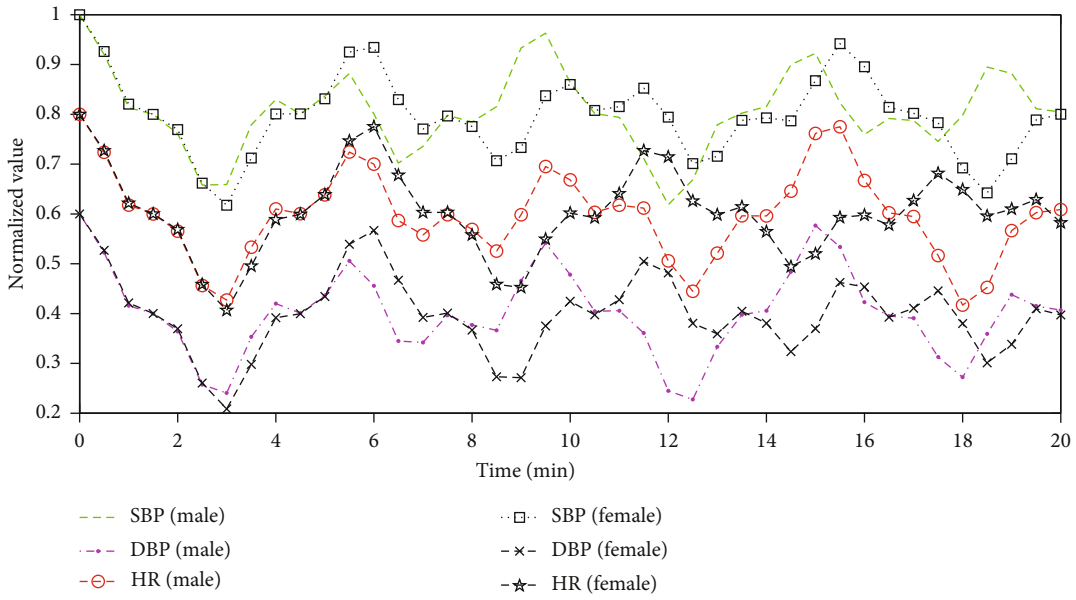

Figure 5: Normalized SBP, DBP, and HR changes of male and female experimenters before and after exercise.

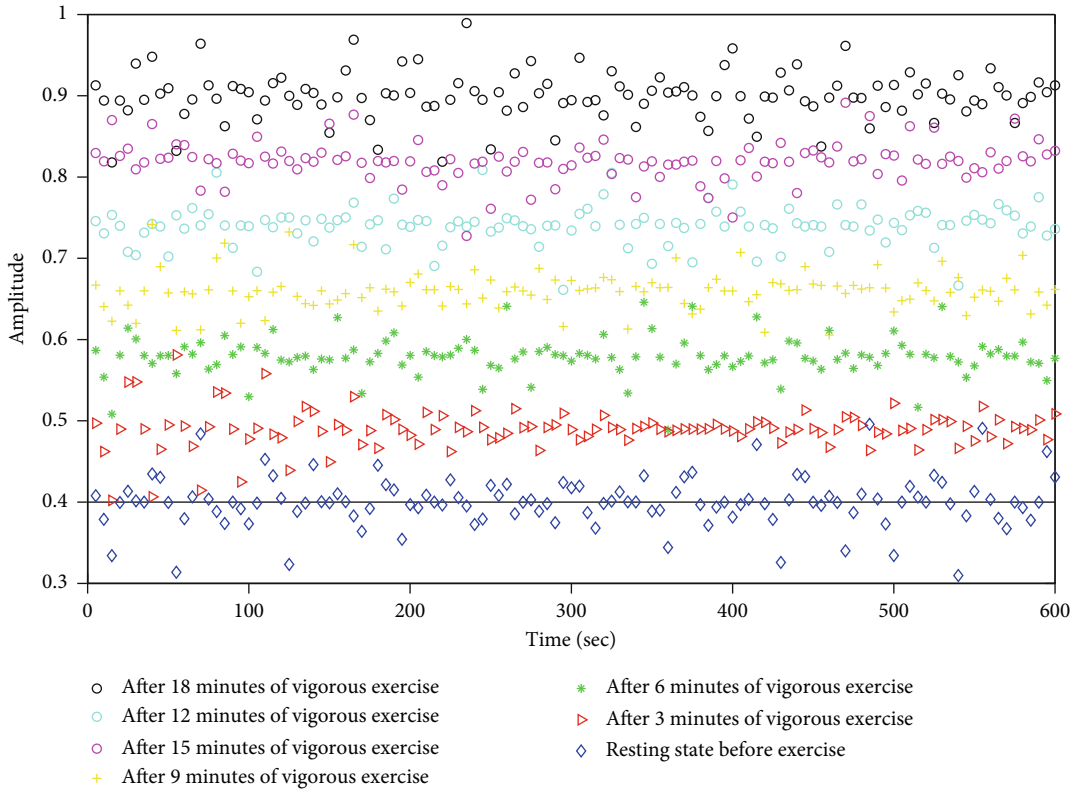

Figure 6: Changes of characteristic points of pulse wave waveform before and after exercise.

monitoring value has not changed significantly. After statistical analysis, it is found that the blood pressure changes of the 24 experimenters can be divided into three categories: (1) after exercise, the systolic blood pressure increased while the diastolic blood pressure decreased; (2) the systolic blood pressure decreased after exercise, while the diastolic blood pressure increased; (3) the diastolic blood pressure increased after exercise, while the diastolic blood pressure did not change significantly.

The two situations (1) and (2) mostly occurred in young male experimenters, and situation (3) occurred more frequently in young female experimenters. Among them, the

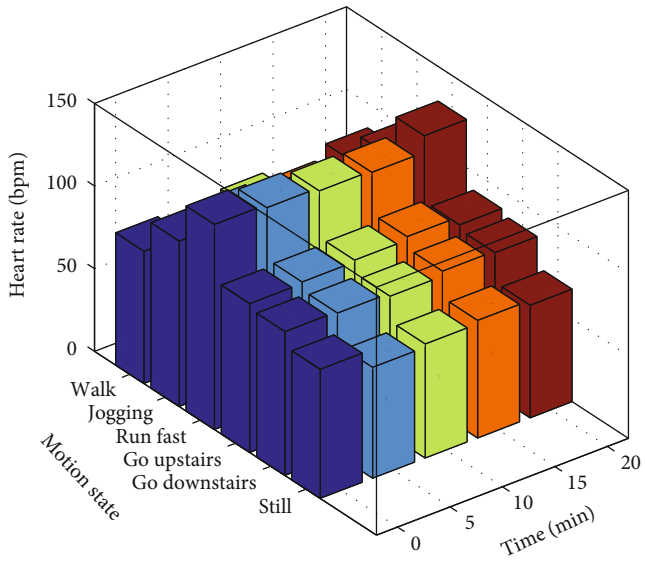

Figure 7: Changes in center rate data during different exercises.

normalized diastolic blood pressure, systolic blood pressure, and heart rate changes of male and female healthy experimenters before and after exercise are shown in Figure 5.

Through analyzing the data, it is found that after 5 minutes of vigorous exercise, the experimenter's diastolic blood pressure dropped from 75 mmHg to 65 mmHg, systolic blood pressure rose from 120 mmHg to 136 mmHg, and heart rate rose from 89 bpm at rest to 130 bpm. After 5 minutes of rest, the experimenter's heart rate began to recover, and the diastolic blood pressure increased, and the systolic blood pressure also began to show a downward trend; after 10 minutes of rest, the diastolic and systolic blood pressure basically returned to their preexercise state. The waveform characteristics of the pulse wave before and after the exercise of this experimenter were collected synchronously as shown in Figure 6. Figure 6 shows the pulse wave waveform feature points in the resting state before exercise and the distribution of waveform feature points after strenuous exercise.

It can be seen from the pulse wave waveform that the wave crest becomes narrower, the pulse rate increases, and the myocardial contractility is strengthened, resulting in an increase in the heart rate. Therefore, it can be seen that exercise leads to faster heart rate, increased myocardial contractility, increased cardiac output, and a certain increase in systolic blood pressure. After exercise, the vascular muscles relax, the peripheral blood vessels dilate, the diameter of the blood vessels increases, and the resistance decreases, which leads to a decrease in diastolic blood pressure. However, in the test, it was also found that after strenuous exercise of the same intensity, the blood pressure of some experimenters was opposite to the above phenomenon. Compared with the resting state before exercise, the systolic blood pressure decreased to a certain extent, and the diastolic blood pressure increased.

4.3. Motion Recognition and Monitoring Incorporating Multiple Physiological Characteristic Parameters. In this section, the physiological data and acceleration data of 12 people standing, squatting, jumping, walking, running, going upstairs, and going downstairs were collected. All 12 people were healthy and free of cardiovascular disease. There was no disease and no disease in the week before the test. We take medication records, and they sleep well and did not stay up late three days before the test. We collect acceleration data worn on the waist of a person wearing physiological signal measurement equipment during exercise. The data includes ECG signals, blood pressure data, and body temperature data.

Before the measurement of each set of exercise data, the experimenter should avoid strenuous exercise and maintain a resting state for 5 minutes. It is necessary to correctly wear a belt-type ECG and acceleration sensor, which can collect ECG signals and acceleration data synchronously, and correctly wear a finger clip blood pressure measuring instrument, which can realize the measurement of blood pressure data during exercise. We perform zero calibration on the acceleration sensor node fixed in the middle of the waist. After being worn correctly, we collected the physiological data and acceleration data of the experimenter in a standing state and recorded it. Each exercise lasts for three minutes, and there are at least 10 rests between the two exercises.

In this section, we will focus on the effectiveness of using physiological data to recognize exercise status. This section introduces blood pressure and heart rate data, mainly discussing the effectiveness of physiological data to improve the performance of exercise recognition. To this end, this section conducts a comparative experiment: only uses acceleration data to recognize sports and uses acceleration data, blood pressure data, and heart rate data to recognize sports. We select 7 experimenters with representative data changes among 12 experimenters for analysis and record the changes of systolic blood pressure, diastolic blood pressure, and heart rate obtained by 7 experimenters after 7 exercises, ECG signal, and acceleration during exercise. In this paper, the RF classification algorithm is used to identify the movement. Figure 7 records the heart rate changes of one of the experimenters during the six exercises. From the data waveform in the figure, it can be seen that the amplitude of the change of the different action data waveforms is obviously different, which verifies the effectiveness of the physiological data to improve the performance of motion state recognition from the data layer.

In this group of experiments, the acceleration data adopts the same set of data samples. The data in the first 20 seconds of the heart rate is eliminated, and the data within 50~230 seconds is selected for analysis. The data collection frequency of the ECG equipment is 360 Hz, and the data collection frequency of the acceleration sensor is 60 Hz. The sample data is intercepted for 5 seconds. There are 4000 sampling points for ECG data and 220 sampling points for acceleration data. A total of 3000 sets of sample data are obtained. 80% of the data is selected for training and 20% for testing. The results of random forest exercise load status monitoring and recognition are shown in Figure 8. It can be seen from the figure that when

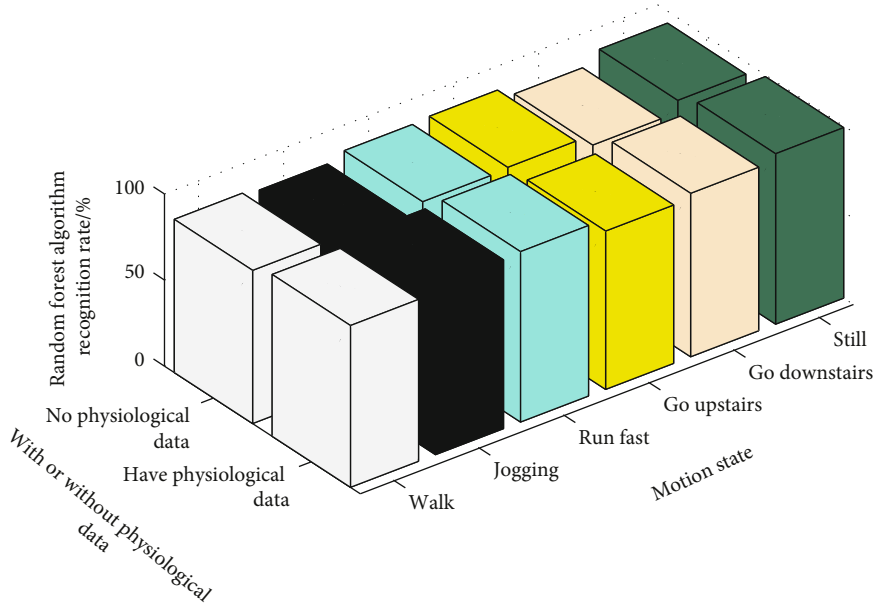

Figure 8: Experimental comparison of the validity of physiological data.

Table 3: Effectiveness classification results.

		Recognition rate (%)	
		Healthy sample	Unhealthy sample
Actual sample	Healthy sample	90.2	6.7
	Unhealthy sample	9.8	93.3

Table 4: Applicability classification results.

		Recognition rate (%)	
		Healthy sample	Unhealthy sample
Actual sample	Healthy sample	91.6	7.9
	Unhealthy sample	8.4	92.1

recognizing motion based on acceleration data, adding physiological data can effectively improve the recognition rate of the motion state.

4.4. Introducing Physiological Parameter Health Monitoring of Exercise Interference

4.4.1. Analysis of the Effectiveness of the Algorithm. We randomly selected a severe fatigue experimenter and collected resting heart rate and blood pressure data in the experimenter's fatigue state. Data was collected every 10 minutes for three minutes each, and a total of 6 sets of data were collected. Resting heart rate and blood pressure data were measured in 6 groups of subjects with unhealthy physiological parameters. In addition, the acceleration data in the stationary state was measured. After the experimenter returned to the awake state, the acceleration data and physiological parameter data in the six exercise states were collected as the data of the healthy group.

We select 216 groups of unhealthy samples (1 person × 6 times × 180 seconds/5 seconds) and select the same number of healthy samples. The classification results are shown in Table 3.

It can be seen from Table 2 that the recognition accuracy of the positive class of the designed classifier is above 89%. For a small sample, the classification recognition rate is ideal. It can be used for doctors or professionals to predict the health status; it can be used to distinguish whether the change of individual physiological parameters is caused by exercise or due to abnormal health of the individual. For example, it can be extended to actual application scenarios to analyze based on a large amount of accurate data.

4.4.2. Analysis of the Applicability of the Algorithm. In this section, the resting heart rate and blood pressure data of 10 severe fatigue experimenters and 4 self-evaluated severe stress experimenters were collected. The data of 14 unhealthy samples were measured to collect the resting heart rate and blood pressure data of the experimenter, as well as the acceleration data in the resting state. The data of the healthy group was collected from the awake state and relaxed state of 14 experimenters as healthy samples. We select 1176 groups of healthy samples (14 people × 7 actions × 60 seconds/5 seconds) and also select 1176 groups of unhealthy samples. The classification results are shown in Table 4.

It can be seen from Table 3 that the recognition accuracy rate of the positive class is above 87%. At the same time, comparing the effectiveness of the algorithm, it can be seen

that the recognition accuracy rate of this group of experiments is slightly lower, but it is also above 87%. Considering the experimenter differences in height, weight, gender, etc., the correct rate is within a controllable range. It shows that the algorithm in this paper is applicable to different experimenters.

5. Conclusion

In this paper, a random forest classification algorithm is selected to classify the motion state. The 27 time-domain and frequency-domain features of the human body's combined acceleration, combined angular velocity, pitch angle, and roll angle are, respectively, extracted to form a 108-dimensional feature vector; when extracting features, a sliding window segmentation method is used for feature extraction. Different actions use appropriate sliding windows to ensure the integrity of each action; the PCA dimensionality reduction method is used to optimize the feature matrix to make the data set cleaner and more concise and improve the calculation performance. This article sets up three sets of experiments to collect data from 24 people to study the changes in exercise heart rate, blood pressure, and body temperature, collect data from 12 people to analyze the effectiveness of fusion of physiological parameters to improve the recognition rate of exercise, and collect data from 14 people to discuss the physiological parameters that introduce exercise interference. The experimental results show that motion recognition with physiological features can effectively improve the recognition rate of motion, and the average recognition rate is increased from 94.8% to 95.7%; the recognition accuracy of the SVM-based blood pressure and heart rate abnormality judgment algorithm is more than 87%. This paper uses a depth camera to obtain depth images to build a human knee joint motion data set and uses neural networks to realize the training of the motion model and the positioning of the main human joints, but there is still a deviation from the motion data obtained by the wearable device. There are two main reasons for this situation: one is that the existing data set is not complete; the other is that the performance of the neural network structure is not strong enough. In order to avoid the shortcomings of the above basic work, the number of samples for the data set can continue to be expanded, including the number of people collected and the number of images, and the network structure can be further optimized. By adjusting the structure and parameter settings, a fast and accurate motion model can be trained. At present, the collection of acceleration sensor data and multiphysiological parameter data cannot be synchronized online and can only be synchronized offline. Next, we will build an integrated motion data and physiological data collection system.

Data Availability

The data used to support the findings of this study are available from the corresponding author upon request.

Conflicts of Interest

The authors declare that they have no known competing financial interests or personal relationships that could have appeared to influence the work reported in this paper.

Acknowledgments

The study was supported by the School of Applied Engineering Henan University of Science and Technology.

References

[1] T. Yang, X. Jiang, Y. Zhong et al., "A wearable and highly sensitive graphene strain sensor for precise home-based pulse wave monitoring," *ACS sensors*, vol. 2, no. 7, pp. 967–974, 2017.

[2] C. Carling, M. Lacome, A. McCall et al., "Monitoring of post-match fatigue in professional soccer: welcome to the real world," *Sports Medicine*, vol. 48, no. 12, pp. 2695–2702, 2018.

[3] L. Djaoui, M. Haddad, K. Chamari, and A. Dellal, "Monitoring training load and fatigue in soccer players with physiological markers," *Physiology & Behavior*, vol. 181, pp. 86–94, 2017.

[4] N. Dey, A. S. Ashour, F. Shi, S. J. Fong, and R. S. Sherratt, "Developing residential wireless sensor networks for ECG healthcare monitoring," *IEEE Transactions on Consumer Electronics*, vol. 63, no. 4, pp. 442–449, 2017.

[5] W. Jeong, J. Song, J. Bae, K. R. Nandanapalli, and S. Lee, "Breathable nanomesh humidity sensor for real-time skin humidity monitoring," *ACS Applied Materials & Interfaces*, vol. 11, no. 47, pp. 44758–44763, 2019.

[6] A. Fornasiero, A. Savoldelli, D. Fruet, G. Boccia, B. Pellegrini, and F. Schena, "Physiological intensity profile, exercise load and performance predictors of a 65-km mountain ultra-marathon," *Journal of Sports Sciences*, vol. 36, no. 11, pp. 1287–1295, 2018.

[7] A. A. Flatt, M. R. Esco, J. R. Allen et al., "Heart rate variability and training load among national collegiate athletic association division 1 college football players throughout spring camp," *The Journal of Strength & Conditioning Research*, vol. 32, no. 11, pp. 3127–3134, 2018.

[8] O. Selmi, H. Marzouki, I. Ouergui, W. BenKhalifa, and A. Bouassida, "Influence of intense training cycle and psychometric status on technical and physiological aspects performed during the small-sided games in soccer players," *Research in Sports Medicine*, vol. 26, no. 4, pp. 401–412, 2018.

[9] H. Kim, J. Lee, and J. Kim, "Electromyography-signal-based muscle fatigue assessment for knee rehabilitation monitoring systems," *Biomedical Engineering Letters*, vol. 8, no. 4, pp. 345–353, 2018.

[10] J. L. Viana, P. Martins, K. Parker et al., "Sustained exercise programs for hemodialysis patients: the characteristics of successful approaches in Portugal, Canada, Mexico, and Germany," *Seminars in Dialysis*, vol. 32, no. 4, pp. 320–330, 2019.

[11] Y. Huo, G. Prasad, L. Atanackovic, L. Lampe, and V. C. M. Leung, "Cable diagnostics with power line modems for smart grid monitoring," *IEEE Access*, vol. 7, pp. 60206–60220, 2019.

[12] P. Sansone, H. Tschan, C. Foster, and A. Tessitore, "Monitoring training load and perceived recovery in female basketball: implications for training design," *The Journal of Strength & Conditioning Research*, vol. 34, no. 10, pp. 2929–2936, 2020.

[13] Y. T. Jao, P. K. Yang, C. M. Chiu et al., "A textile-based triboelectric nanogenerator with humidity-resistant output characteristic and its applications in self-powered healthcare sensors," *Nano Energy*, vol. 50, pp. 513–520, 2018.

[14] O. Postolache, D. J. Hemanth, R. Alexandre, D. Gupta, O. Geman, and A. Khanna, "Remote monitoring of physical rehabilitation of stroke patients using IoT and virtual reality," *IEEE Journal on Selected Areas in Communications*, vol. 39, no. 2, pp. 562–573, 2021.

[15] N. Xing, L. Ji, J. Song et al., "Cadmium stress assessment based on the electrocardiogram characteristics of zebra fish (*Danio rerio*): QRS complex could play an important role," *Aquatic Toxicology*, vol. 191, pp. 236–244, 2017.

[16] A. A. Flatt and D. Howells, "Effects of varying training load on heart rate variability and running performance among an Olympic rugby sevens team," *Journal of Science and Medicine in Sport*, vol. 22, no. 2, pp. 222–226, 2019.

[17] H. Peltonen, S. Walker, A. Lähitie, K. Häkkinen, and J. Avela, "Isometric parameters in the monitoring of maximal strength, power, and hypertrophic resistance-training," *Applied Physiology, Nutrition, and Metabolism*, vol. 43, no. 2, pp. 145–153, 2018.

[18] R. Zacca, R. Azevedo, P. Chainok et al., "Monitoring age-group swimmers over a training macrocycle: energetics, technique, and anthropometrics," *The Journal of Strength & Conditioning Research*, vol. 34, no. 3, pp. 818–827, 2020.

[19] A. S. Martorelli, F. D. de Lima, A. Vieira et al., "The interplay between internal and external load parameters during different strength training sessions in resistance-trained men," *European Journal of Sport Science*, vol. 21, no. 1, pp. 16–25, 2021.

[20] D. Conte, N. Kolb, A. T. Scanlan, and F. Santolamazza, "Monitoring training load and well-being during the in-season phase in national collegiate athletic association division I men's basketball," *International Journal of Sports Physiology and Performance*, vol. 13, no. 8, pp. 1067–1074, 2018.

[21] L. T. Starling and M. I. Lambert, "Monitoring rugby players for fitness and fatigue: what do coaches want?," *International Journal of Sports Physiology and Performance*, vol. 13, no. 6, pp. 777–782, 2018.

[22] M. J. Buller, A. P. Welles, and K. E. Friedl, "Wearable physiological monitoring for human thermal-work strain optimization," *Journal of Applied Physiology*, vol. 124, no. 2, pp. 432–441, 2018.

[23] M. M. Kolokoltsev, S. S. Iermakov, and K. Prusik, "Motor skills and functional characteristics of students of different somatotypes," *Physical Education of Students*, vol. 22, no. 1, pp. 31–37, 2018.

[24] M. Zhu, Q. Shi, T. He et al., "Self-powered and self-functional cotton sock using piezoelectric and triboelectric hybrid mechanism for healthcare and sports monitoring," *ACS Nano*, vol. 13, no. 2, pp. 1940–1952, 2019.